Evaluation of spectroscopic properties of Yb^{3+}-doped glasses

Xuelu Zou and Hisayoshi Toratani
Research and Development Center, HOYA Corporation Musashino 3-3-1, Akishima-shi, Tokyo 196, Japan
(Received 11 May 1995)

The absorption and emission properties of numerous glasses doped with Yb^{3+} ions have been investigated. The emission cross sections have been evaluated using the measured absorption spectra and principle of reciprocity, and again using the Fuchtbauer-Ladenburg formula. Agreement between the two methods is typically within 25% for most materials. The spectroscopic properties of the $^2F_{7/2}$-$^2F_{5/2}$ transition have been found to be very sensitive to the Yb^{3+} site environment as well as an hypersensitive transition, and their values increase as the asymmetry of the Yb^{3+} site becomes higher. High asymmetry of the Yb^{3+} site is essentially caused not only by large difference in the cationic field strengths between network formers around the [YbO_6] coordination sphere, but also by difference in the coordination numbers of oxygens surrounding network formers that are associated with the Yb^{3+} through the oxygens. A system of Yb:(15-25)P_2O_5-(10-20)Nb_2O_5-(0-15)B_2O_3-(48-55)RO (R=Mg, Ca, Sr, Ba, and Zn) glasses which possess higher asymmetry of Yb^{3+} ligands has been developed. These glasses exhibit the most useful laser properties, and are expected to be substantially superior to Yb:SiO_2 and Yb:ZBLAN glass fiber lasers in many key spectroscopic parameter values.

I. INTRODUCTION

Laser fiber devices based on Pr^{3+}-doped fluoride glasses have been recently receiving increasing attention because of their potential application as amplifiers in the 1.3 μm communication window.[1–3] The problem of optical amplification around 1.3 μm in Pr^{3+}-doped fluoride fibers raises the question of the pump source, the wavelength of which must be chosen to be at 1.02 μm to obtain efficient amplification. Since the low absorption cross section and the high background losses usually encountered in fluoride fibers, the pump power required to obtain a gain rapidly increases as the pump wavelength shifts from its optimum value of 1.02 μm. Powerful laser diodes at about 1.017 μm are now available, and 42 dB net gain has already demonstrated by pumping with four laser diodes.[4] Another way to populate the $^1G_4$ level of Pr^{3+} is to codope with Yb^{3+} and to use the efficient energy transfer from $Yb^{3+}(^2F_{5/2})$ to $Pr^{3+}(^1G_4)$. The pump wavelength range can then be extended down to ~0.85 μm, making possible the use of cheap powerful laser diodes.[5–7] Unfortunately, the experiments have not, up to now, given better results than direct pumping of Pr^{3+}.

Clearly, Yb^{3+} is a good candidate as a pump source for Pr^{3+}, because it has a single transition emitting around 1.02 μm and negligible nonradiative relaxation rate. Extensive work on laser operation of Yb^{3+} in silica fibers has been published and the possibility of using Yb^{3+} fiber laser as a source to pump Pr^{3+} has also been investigated.[8–11] A tunable range from 1.01 to 1.16 μm has been reported for Yb^{3+}-doped silica fibers, but with only low output power at 1.02 μm. With usual laser cavity, large output powers can be obtained only at 1.04 μm which is not optimum for pumping Pr^{3+}, because of the shape of the emission spectrum of Yb^{3+} in silica. The purpose of this work is to survey the optical properties of Yb^{3+}-doped numerous glasses in order to assess their potential laser performance in diode pumped systems and to identify Yb-gain media potentially superior to Yb^{3+}-doped silica glass. Our interest is to identify specific candidates for Yb-laser operation.

II. EXPERIMENT

Glasses used in this study were prepared with highly purified raw materials. The glasses were melted in platinum crucibles in air for 1.5–2 h at 1050–1450 °C and then annealed at their transition temperatures. The batch compositions of the glasses are listed in Table I. Samples for the optical property measurements were cut and polished by the same process to the size of 25×25×5 mm^3.

Absorption spectra were recorded on a Hitachi-330 spectrophotometer at room temperature. The emission spectra were measured by exciting the samples with light from a diode laser operating at 0.98 μm. The light was chopped at 80 Hz and focused on the 25×25 mm^2 face of the samples. A position 0.2 mm from an edge was excited to minimize the reabsorption of emission. Average beam size of the light from the laser diode through the sample was about 0.2 mm^2. The emission from the sample was focused onto a monochrometor and detected by a Ge detector. The signal was intensified with a lock in amplifier and processed by a computer. The relative errors in these emission measurements are estimated to be <5%. The emission lifetimes were measured by exciting the samples with a Ti-sapphire laser operating at 968 nm and the emission was detected with a S-1 photomultiplier tube. The emission decay curves were recorded and averaged with a computer controlled transient degitizer. To reduce the effects of radiation trapping due to the reabsorption and impurity absorption, the samples used in the lifetime measurements were cut and polished to the size of 5×5×0.3 mm^3. The errors in these measurements are estimated to be <12%.

TABLE I. Compositions of Yb^{3+}-doped various glasses (mol %).

Glass	Glass systems
AY-1	$31.17Al_2O_3$-47.01CaO-10.41MgO-10.41BaO-$1Yb_2O_3$
PSB-1	$40P_2O_5$-$19SiO_2$-$40B_2O_3$-$1Yb_2O_3$
FCD-10	$5.3P_2O_5$-$34.8AlF_3$-$4YF_3$-50.6(MgF_2+CaF_2+SrF_2+BaF_2)-5.3NaF-$2YbF_3$
LSY-8	$49.8SiO_2$-$4.91Al_2O_3$-$23.92Li_2O$-$12.07Na_2O$-$9.43SrO$-$1Yb_2O_3$
PN-*X*	(45-*X*)P_2O_5-*X*Nb_2O_5-24CaO-10SrO-20BaO-$1Yb_2O_3$ (*X*=0,5,10,15,20,22.5)
PNB-*X*	(36-*X*)P_2O_5-*X*Nb_2O_6-$13B_2O_3$-20ZnO-15SrO-15BaO-$1Yb_2O_3$ (*X*=0,5,10,15,18,20)
PNK-*X*	(42.5-*X*)P_2O_5-(42.5-*X*)Nb_2O_5-*X*K_2O-$1Yb_2O_3$ (*X*=25,30,35,40)
NPY-*X*	$35P_2O_5$-$28B_2O_3$-36*X*O-$1Yb_2O_3$ (*X*=Mg,Ca,Sr,Ba,Zn)
BS-*X*	*X*SiO_2-(50-*X*)B_2O_3-10MgO-15CaO-19SrO-5BaO-$1Yb_2O_3$ (*X*=5,15,20,25,30,35)
BG-*X*	*X*GeO_2-(50-*X*)B_2O_3-10MgO-15CaO-19SrO-5BaO-$1Yb_2O_3$ (*X*=5,15,20,25,30)
BN-*X*	$5SiO_2$-(45-*X*)B_2O_3-*X*Nb_2O_5-19CaO-10SrO-20BaO-$1Yb_2O_3$ (*X*=5,10,15)
BNS-*X*	*X*SiO_2-(35-*X*)B_2O_3-$15Nb_2O_5$-19CaO-10SrO-20BaO-$1Yb_2O_3$ (*X*=0,10,15,20,25)

III. EXPERIMENTAL RESULTS

A. Absorption and emission cross sections

The potential performance of an Yb^{3+}-doped glass laser may be assessed from the emission and absorption properties. The important spectroscopic parameters required include the effective emission and absorption cross sections of the $^2F_{7/2}$-$^2F_{5/2}$ transition and the upper laser level lifetimes of Yb^{3+}. The emission cross sections are determined using either the method of reciprocity or the Fuchtbauer-Ladenburg formula and we have carried out both determinations where sufficient information is available. On the basis of the reciprocity method described by McCumber.[12] The emission cross section, σ_{emi} of Yb^{3+} in a strongly phonon coupled system can be well calculated from the measured absorption cross section, σ_{abs}, i.e.,

$$\sigma_{emi}(\lambda)=\sigma_{abs}(\lambda)\,\frac{Z_l}{Z_u}\,\exp\left(\frac{E_{ZL}-hc\lambda^{-1}}{kT}\right), \qquad (1)$$

where Z_l, Z_u, k, and E_{ZL} represent the partition functions of the lower and the upper states, Boltzman's constant, and the zero line energy which is defined to be the energy separation between the lowest components of the upper and lower states, respectively. In the high temperature limit, the ratio of Z_l/Z_u simply becomes the degeneracy weighting of the two states. This approximation is available for the Yb^{3+}-doped glasses, since only one broad absorption band corresponding to the $^2F_{7/2}$-$^2F_{5/2}$ transition was observed even at low temperature, and so that the levels can be represented as two continuous sets of levels.[13] Another parameter, E_{ZL} can be determined by matching the magnitude of actual emission spectrum to that of the derived emission result of Eq. (1), since the derived and actual emission spectra agree reasonably well in line shape.[14]

While we have chosen the reciprocity method of (1) to obtain the emission cross sections, we will use the Fuchtbauer-Ladenburg equation to calculate them as a method of checking the reasonableness of our results. The Fuchtbauer-Ladenburg equation has been commonly used by researchers, and is grounded in the fundamental aspects of the Einstein A and B coefficients. The form of the equation is[14]

$$\sigma_{emi}=\frac{\lambda^4 A_{rad}}{8\pi c n^2}\,q(\lambda), \qquad (2)$$

where $q(\lambda)$ is the normalized line shape function of the $^2F_{5/2}$-$^2F_{7/2}$ transition of Yb^{3+}, n is the refractive index, and c is the velocity of light, and A_{rad} is the spontaneous-emission probability which can be calculated from

$$A_{ad}=\frac{8\pi c n^2(2J'+1)}{\lambda_p^4\rho(2J+1)}\int k(\lambda)d\lambda, \qquad (3)$$

where ρ is the concentration of Yb^{3+} ions, J and J' are the total momentums for the upper and lower levels, $k(\lambda)$ is the absorption coefficient, and λ_p is the absorption peak wavelength.

Utilizing the above equations [(1)–(3)] we calculated the emission cross sections of Yb^{3+} in the given glasses. The glasses were selected which allow the study of the Yb^{3+} ion in a variety of crystal field environments in order to characterize the range of spectroscopic properties and to assess their potential laser performance in diode laser pumped systems. The measured absorption and the derived emission spectra of Yb^{3+} are presented for some glasses in Fig. 1 with absolute cross section scales. The data at the wavelengths longer than about 1.05 μm were fitted by Gaussian function using the measured bandwidths of emission spectra. It can be seen from Fig. 1 that the absorption and emission spectra are

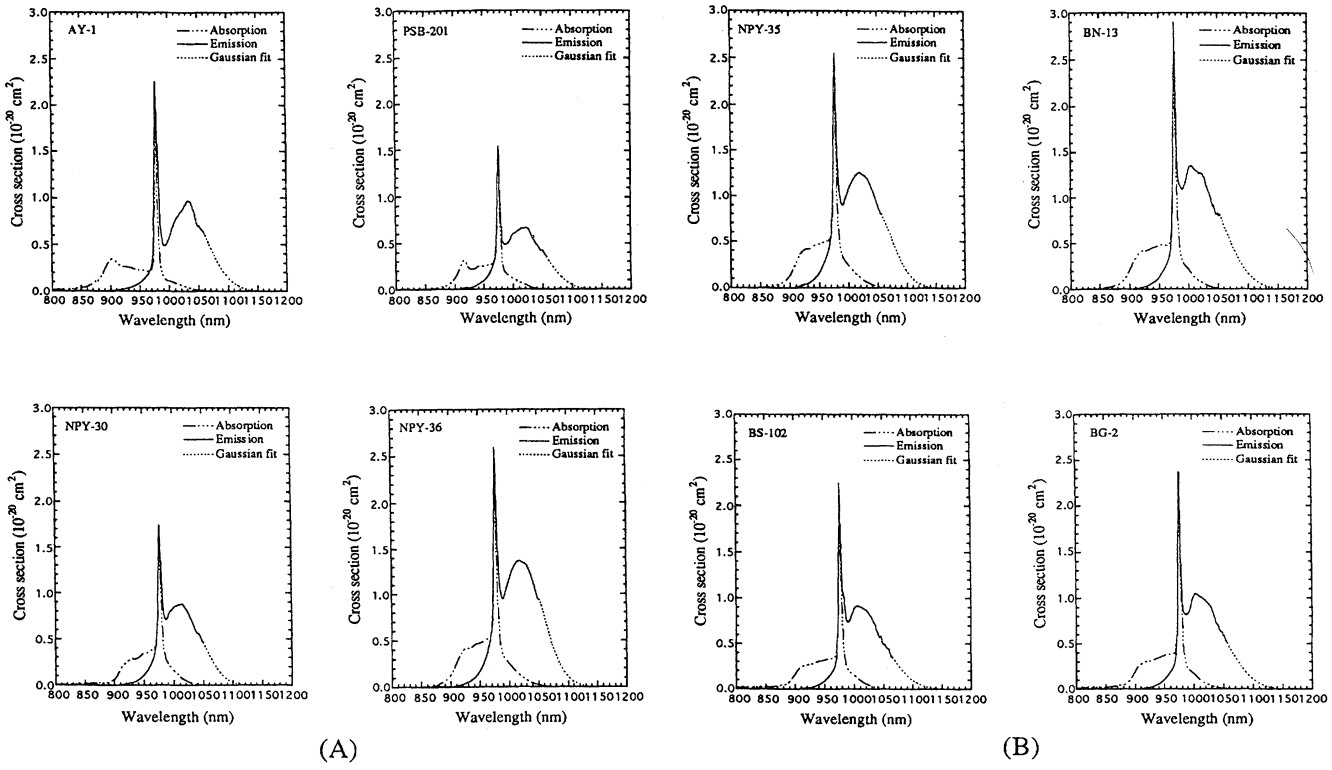

FIG. 1. The measured absorption and the derived emission spectra of Yb^{3+} in various glass hosts with absolute cross section scales. (a) Yb^{3+}-doped AY-1, PSB-1, PN-0, and PN-20 glasses; (b) Yb^{3+}-doped PNB-18, BN-15, BS-20, and BG-5 glasses.

generally in good agreement, in which the same features appear in both the spectra and have similar widths. We believed that the essential features in the spectra are adequately resolved. The absorption peak wavelengths, corresponding to the energy separation of the lowest crystal field components of the ground and excited states, are situated in narrow ranges of 975–978 nm for the given glasses. Although the values of absorption and emission cross sections are obviously different, the line shapes of the emission spectra are sufficiently similar for the glasses so that the emission peak wavelengths are situated in narrow wavelengths of 1.00–1.02 μm except the aluminate glass. This behavior implies that the Yb^{3+} ions most likely occupied at the same sites, into which the glass network modifiers are generally incorporated.

The utility of the data in Fig. 1 is, in part, derived from the extensive nature of the survey, in which a single methodology of determining the cross sections has been uniformly applied to a wide range of materials. As a result the data characterizing various materials may be conveniently compared, and are expected to have an enhanced level of relative accuracy. It is noteworthy, however, that the samples utilized were not always available with the optimum concentration, size, and optical quality. Thus the Fuchtbauer-Ladernburg equation was utilized to determine the emission cross sections for assessing the reasonableness of calculated results by the method of reciprocity. The calculated results are listed in Table II where several of parameters that are required for the calculation and the measured lifetimes are also listed. The maximum discrepancies between two values of the emission cross sections derived by both the methods are found to be <25%. This error represents the combined uncertainty of the absorption and emission line shape functions. In fact, based on the cumulative errors associated with the spectra, energy level assignments and Yb^{3+} concentrations, it is conservatively estimated that the emission cross sections are accurate to about 20%.

B. Compositional dependence of emission cross sections

Upon inspection of data in Table II, it is seen that the emission cross sections of Yb^{3+} in the systems are strongly affected by the glass network formers, but not by the network modifiers and their concentrations. For instance, if the network formers such as P^{5+}, Si^{4+}, and Ge^{4+} in the systems are substituted by Nb^{5+} that possesses larger polarizability and ionic radius, or by B^{3+} which can be coordinated with either three or four oxygens, the emission cross sections increase as shown in Fig. 2. By contrast, when either the network modifiers of MgO, CaO, SrO, ZnO, and BaO are replaced by each other in the P_2O_5-B_2O_3-RO(R=Mg, Ca, Sr, Zn, and Ba) system, or the modifier concentration of K_2O is increased in the P_2O_5-Nb_2O_5-K_2O system, the spectroscopic properties of Yb^{3+} are sufficiently similar so that the nearly equal values of the emission cross sections were observed. Similarly, the nearly same values of the emission cross sections were also observed in SiO_2 and LSY-8 glasses due to both the glasses being formed by the same network formers. It indicates that the Yb^{3+} ions are essentially coordinated with such oxygens which are associated with the network formers.

However, it should be noteworthy that the emission cross sections of Yb^{3+} in the glass composed of the pure network formers of P_2O_5, B_2O_3, and SiO_2(PSB-1) is much smaller than those of the glasses prepared with both the network formers and modifiers. This behavior has been evidenced based on the scanning electron microscopy observations to ascribe to the phase separation in PSB-1 glass, in which the Yb^{3+} ions are rich in a glass phase containing the same type of network formers. In this case, most of the Yb^{3+} ions are only surrounded by the nearly same structural units. As more than 45% of network modifiers such as MgO, CaO, SrO, and BaO are incorporated into the systems containing more than

TABLE II. Spectroscopic properties of Yb^{3+} in glass hosts.

Glass	n_d	λ_0 (nm)	τ_f (msec)	σ_{emi} (10^{-20} cm^2)	β_{min}	I_{sat} (kW/cm^2)	I_{min} (kW/cm^2)
AY-1	1.692 46	1.035	1.015	0.96	0.0963	11.62	1.12
PSB-1	1.526 19	1.022	0.691	0.66	0.0884	22.11	1.95
SiO_2[a]	1.456 10	1.032	0.800	0.55	0.0833	15.41	1.28
LSY-8	1.573 90	1.012	1.04	0.56	0.0785	22.23	1.75
ZBLAN	1.500 60	1.001	1.810	0.46	0.1000	11.24	1.12
FCD-10	1.444 80	1.012	2.12	0.61	0.1001	8.65	0.87
PN-0	1.586 04	1.014	1.315	0.94	0.0718	10.29	0.74
PN-5	1.639 68	1.016	1.249	1.00	0.0695	10.17	0.71
PN-10	1.697 14	1.018	1.160	1.12	0.0664	9.77	0.65
PN-15	1.759 15	1.018	1.120	1.21	0.0632	9.30	0.59
PN-20	1.821 23	1.019	1.090	1.36	0.0578	8.89	0.51
PN-22.5	1.852 34	1.019	0.945	1.35	0.0595	9.90	0.59
PNB-0	1.602 33	1.018	1.360	0.89	0.0593	9.67	0.57
PNB-5	1.658 82	1.018	1.314	0.99	0.0593	9.17	0.54
PNB-10	1.719 24	1.019	1.281	1.11	0.0575	8.37	0.48
PNB-15	1.784 45	1.020	1.260	1.20	0.0561	7.90	0.44
PNB-18	1.814 20	1.020	1.150	1.31	0.0562	7.99	0.45
PNB-20	1.852 37	1.020	0.964	1.33	0.0549	9.29	0.51
PNK-25	1.768 66	1.012	0.964	0.81	0.0935	15.55	1.45
PNK-30	1.733 82	1.014	1.233	0.81	0.0873	12.17	1.06
PNK-35	1.717 43	1.015	1.275	0.82	0.0808	11.59	0.94
PNK-40	1.677 08	1.016	1.360	0.83	0.0812	11.03	0.90
NPY-Mg	1.534 65	1.018	0.99	0.87	0.0679	12.23	0.83
NPY-Ca	1.570 94	1.018	0.98	0.83	0.0814	13.39	1.09
NPY-Sr	1.577 96	1.019	0.98	0.85	0.0598	13.84	0.83
NPY-Ba	1.596 82	1.019	0.99	0.81	0.0581	13.75	0.80
NPY-Zn	1.568 56	1.018	1.00	0.83	0.0697	13.36	0.93
BS-5	1.634 31	1.012	0.900	1.11	0.0805	10.14	0.82
BS-15	1.636 83	1.012	0.820	1.00	0.0841	12.49	1.05
BS-20	1.637 35	1.012	0.870	0.96	0.0861	12.36	1.06
BS-25	1.637 19	1.012	0.890	0.93	0.0861	12.66	1.09
BS-30	1.637 22	1.012	0.960	0.91	0.0850	12.47	1.06
BS-35	1.636 67	1.012	1.001	0.89	0.0854	12.73	1.09
BG-5	1.642 03	1.014	0.920	1.10	0.0767	9.42	0.72
BG-15	1.660 70	1.014	0.880	1.10	0.0756	10.31	0.78
BG-20	1.669 58	1.014	0.830	1.10	0.0742	9.94	0.74
BG-25	1.679 17	1.014	0.890	1.05	0.0757	10.41	0.79
BG-30	1.689 06	1.014	0.890	1.06	0.0756	10.04	0.76
BN-5	1.710 2	1.015	0.860	1.09	0.0600	11.92	0.72
BN-10	1.771 10	1.015	0.790	1.18	0.0615	11.48	0.71
BN-15	1.829 26	1.015	0.760	1.33	0.0586	10.88	0.64
BNS-0	1.826 82	1.015	0.710	1.39	0.0595	10.85	0.65
BNS-10	1.832 20	1.015	0.730	1.30	0.0594	11.68	0.69
BNS-15	1.834 81	1.015	0.770	1.23	0.0600	11.92	0.71
BNS-20	1.836 89	1.015	0.770	1.20	0.0610	12.43	0.76
BNS-25	1.838 42	1.015	0.780	1.15	0.0628	12.69	0.80

[a]The data are reported by Allain *et al.* (Ref. 10).

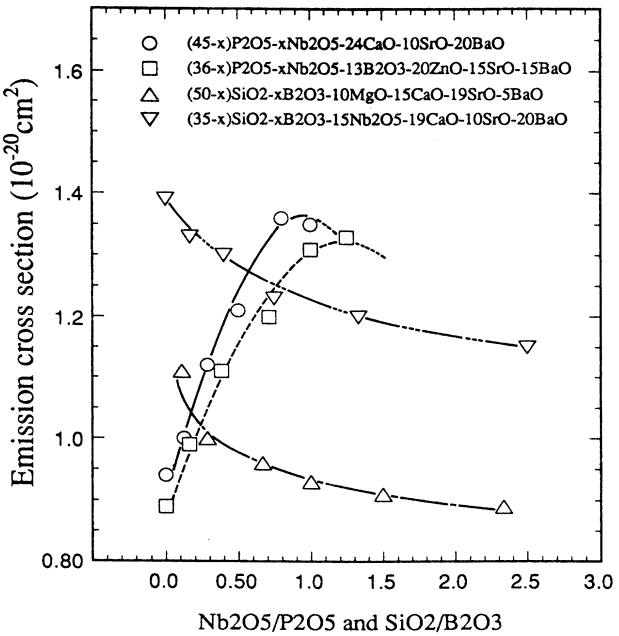

FIG. 2. Compositional dependences of emission cross sections of Yb^{3+} in the given glasses doped with 1 mol %Yb_2O_3.

two network formers, the observable phase separation in the systems does not occur, so that the $[SiO_4]$, $[PO_4]$, $[BO_4]$, $[BO_3]$, and $[GeO_4]$ structural units are homogeneously distributed around Yb^{3+} ions, and thus causes the emission cross sections of Yb^{3+} to increase.

C. Laser performance parameters

The complete assessment of Yb^{3+}-doped laser glasses involves several parameters impacting laser performance. First important laser parameter, $\beta_{\min}$, is defined as the minimum fraction of Yb^{3+} ions that must be excited to balance the gain exactly with the ground state absorption at laser wavelength, λ_0. The $\beta_{\min}$ parameter is of crucial importance for quasi-four-level systems such as an Yb^{3+}-doped glass. The quantity of $\beta_{\min}$ is simply given by[15]

$$\beta_{\min}=\frac{\sigma_{\mathrm{abs}}(\lambda_0)}{\sigma_{\mathrm{emi}}(\lambda_0)+\sigma_{\mathrm{abs}}(\lambda_0)}. \tag{4}$$

When the $\beta_{\min}$ fraction of the Yb^{3+} population is excited, the upward and downward transition rates are equal, and the Yb glass essentially becomes transparent at λ_0, such that there is neither gain nor loss for a weak laser probe beam. Since the emission and absorption cross sections are related by the reciprocity, the $\beta_{\min}$ parameter can be also rewritten as

$$\beta_{\min}=\left\{1+\frac{Z_l}{Z_u}\exp\left(\frac{E_{\mathrm{ZL}}-hc\lambda_0^{-1}}{kT}\right)\right\}^{-1}. \tag{5}$$

Another important parameter that characterizes the pumping dynamics is the pump saturation intensity, I_{sat}, which requires an accurate measure of the absorption cross section at laser pump wavelength, λ_p, and the emission lifetime, τ_f, of Yb^{3+}. The form of the relationship is

$$I_{\mathrm{sat}}=\frac{hc}{\lambda_p\sigma_{\mathrm{abs}}(\lambda_p)\tau_f}, \tag{6}$$

where hc/λ_p is the pumping energy. Since InGaAs diode laser sources are regarded as peak-power-limited devices, clearly, a larger pump cross section and a longer emission lifetime lead to a low value of I_{sat} and to accumulate a greater population inversion for a peak power.

Finally, $I_{\min}$ is a parameter which evaluates the minimum absorbed pump intensity. This parameter is required for threshold to be reached. $I_{\min}$ takes into account both the absorption and emission properties and is calculated by the following expression:

$$I_{\min}=\frac{hc}{\lambda_p\sigma_{\mathrm{abs}}(\lambda_p)\tau_f}\left\{1+\frac{Z_l}{Z_u}\exp\left(\frac{E_{\mathrm{ZL}}-hc\lambda^{-1}}{kT}\right)\right\}^{-1}. \tag{7}$$

We have calculated the minimum fraction of Yb^{3+} ions, the pump saturation intensity, and the minimum pump intensity utilizing Eqs. (5), (6), and (7) and given them in Table II. The pump saturation intensities and the minimum pump intensities occur in range of 7–23 (kW/cm^2), and 0.4–2.0 (kW/cm^2) for the glasses, respectively. For the laser performance, the $\beta_{\min}$ parameter addresses the effect of the resonant absorption loss of Yb^{3+} at λ_0, and the $I_{\min}$ parameter provides a useful measure of the ease by which the Yb^{3+}-doped glass can be bleached. It is desirable for reducing both the parameters to give rise to a minimum amount of the absorbed pump power required for threshold to be reached. Since the minimum pump intensity takes into account both absorption and emission properties, in brief, favorable spectroscopic parameters, which lead to more attractive laser performance, should include a large emission cross section at λ_0, a large absorption cross section at λ_p, and a long lifetime of the upper laser level. It is therefore expected that the minimum absorbed pump power should decrease as the product of $\sigma_{\mathrm{abs}}(\lambda_p)$, $\sigma_{\mathrm{emi}}(\lambda_0)$, and τ_f increases as shown in Fig. 3.

In scanning the data in Table II, it is predicted that the Yb:PNB-18 and Yb:PN-20 will require only minimal pump energy for threshold to be reached, since $I_{\min}$=0.45–0.51 kW/cm^2 which are smaller than that of Yb:SiO_2, such that useful architectures employing InGaAs diode laser pumping will be easily achievable. The emission cross sections are about 1.31 and 1.36×10^{-20} cm^2 and the lifetimes are about 1.15 and 1.09 msec for both the materials. They are all substantially superior to those for the Yb:SiO_2 and ZBLAN glass lasers.

D. Evaluation of the threshold pump power for Yb-fiber laser

In order that the critical inversion may be continuously maintained for Yb^{3+} fiber laser operation, the loss by spontaneous emission from the upper laser level must be supplied by the pump energy. As a result, we obtain for the absorbed pump power, P_{abs}, needed to compensate for population loss of the laser level by spontaneous emission

$$P_{\mathrm{abs}}=\frac{hcn_2(\lambda_0)}{\eta\lambda_p\tau_f}, \tag{8}$$

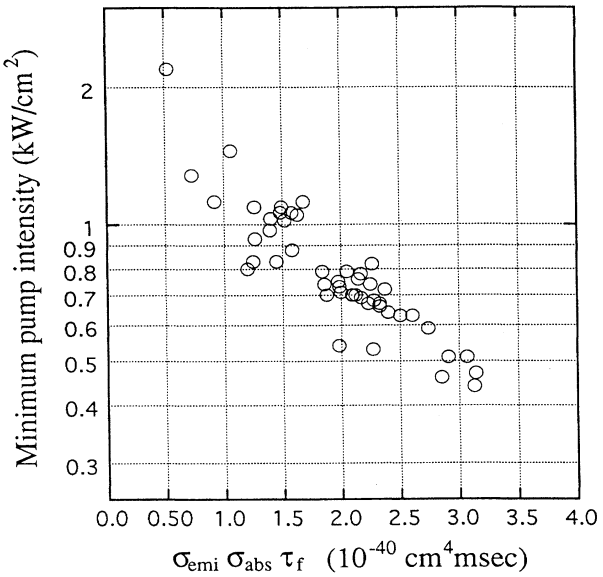

FIG. 3. A plot of minimum pump intensity versus the product of absorption cross section, σ_{abs} emission cross section, σ_{emi}, and emission lifetime, τ_f, for Yb^{3+}-doped glasses.

where η is the efficiency factor of pumping and can be defined as the quantum efficiency, η_q, of Yb^{3+} and $n_2(\lambda_0)$ is the population inversion at λ_0 and can be written as

$$n_2(\lambda_0)=\frac{\pi\phi^2}{4}L\rho\chi(1-\delta), \tag{9}$$

where L and ϕ represent the fiber length and the Yb^{3+} dopant diameter, δ is the excitation loss due to the background loss, which can be evaluated from the measured transmission loss spectrum for the fiber without doping of Yb^{3+}, and χ is the mean fraction of excited Yb^{3+} ions along the fiber axis and can approximately be expressed by the β_{min} parameter at threshold. Then, the minimum pump power which must be absorbed to maintain the threshold inversion at laser wavelength, λ_0, can be calculated with the expression

$$P_{abs}=\frac{hcL\rho\pi\phi^2(1-\delta)}{4\eta_q\lambda_p\tau_f}\left\{1+\frac{Z_l}{Z_u}\exp\left(\frac{E_{ZL}-hc\lambda^{-1}}{kT}\right)\right\}^{-1}. \tag{10}$$

Theoretically, since Yb^{3+} has only one excited state and no significant multiphonon relaxation, the differential quantum efficiency should be equal to 1. Using Eq. (10), therefore, the threshold pump powers were calculated to be about 6.91 mW for Yb:SiO_2 and 4.89 mW for Yb:PNB-18 fiber lasers. In these calculations, the fibers which had a core of 2.5 μm diameter doped with 1100 ppm of Yb^{3+} and a refractive index difference of 24×10^{-3} were used. Allain *et al.*[11] have reported the measured threshold pump power of 7.5 mW for the same type of Yb:SiO_2 glass fiber laser. This measured value is in good agreement with our calculated one, proving that the model established here can accurately evaluate some important parameters characterizing the laser performance of an Yb-glass laser from the measured spectroscopic properties.

IV. DISCUSSION

Yb^{3+}-doped various glasses exhibits a significant range of emission cross sections, 0.46 to 1.37×10^{-20} cm^2, which suggests the local environments of the Yb^{3+} sites characterized by both the Yb^{3+} site symmetry and its bonding characteristic must impact this property. For example, the glasses with larger emission cross sections, such as P_2O_5-Nb_2O_5-RO, P_2O_5-Nb_2O_5-B_2O_3-RO, and B_2O_3-Nb_2O_5-SiO_2-RO systems, usually contain more than two network formers and high content of modifiers. However, the glasses that were prepared by one type of network formers with and without modifiers generally possess smaller emission cross sections. This compositional dependence may be qualitatively understood on the basis of the following model. At a given oxide glass with 1 mol % Yb^{3+}, the Yb^{3+} ion is in a network modifier position surrounded by six oxygen ions which are, on the other hand, associated with the network former ions. When such a $[YbO_6]$ coordination sphere is surrounded by the network formers which possess different cationic field strengths, polarizabilities, and coordination numbers of oxygens, the Yb^{3+} ion must be situated into an asymmetrical coordination sphere of oxygens. For example, in the P_2O_5-Nb_2O_5-B_2O_3-RO system, the Yb^{3+} ions may be bonded with the oxygens that are associated with the network formers as possible types of

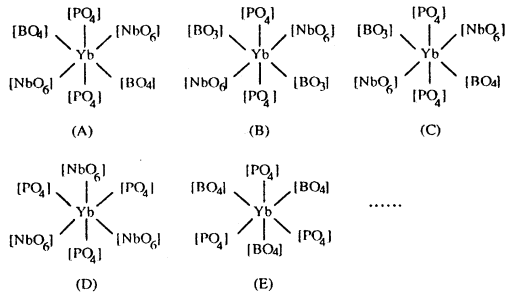

where the niobium ions take sixfold coordination[16] and the other network former ions are considered to be three and fourfold coordinated by oxygens as shown in the draft numbers. Since the cationic field strengths of the network formers are significantly different as shown in Table III, the $[PO_4]$-Yb, $[BO_4]$-Yb, $[BO_3]$-Yb, and $[NbO_6]$-Yb bond distances must be different and thus causes the symmetry of the coordination sphere of oxygens around Yb^{3+} to be broken. Obviously, the addition of the Nb^{5+} and B^{3+} network formers into the given systems not only varies the bonding characteristic of Yb-O but also distorts the symmetry of sixfold coordinated Yb^{3+} site. For the single network former system, however, the Yb^{3+} ions may be incorporated into nearly centrosymmetric sites, since the coordination sphere is only surrounded by the same network former ions. Although the addition of modifiers into such single-former system can be associated with a general loosening of the oxygen ions around Yb^{3+} and then leads to an increase in the covalency of Yb-O bond, the nearly equal values of the emission cross sections were actually observed for both the single-former systems with and without modifiers (due to the similar symmetries of Yb^{3+} site). It suggests that the effect of Yb-O bonding characteristics can be negligible and the difference

TABLE III. Physical properties of glass network former cations in the given systems.

Network-former cations	Cationic radius, r (Å)	Coordination number, N	Cationic field strength, Z/Nr[a]	Average cationic field strength
B^{3+}	0.21	3	4.76	
B^{3+}	0.22	4	3.41	$[BO_{3,4}]$:4.08
P^{5+}	0.33	4	3.79	$[PO_4]$:3.79
Si^{4+}	0.40	4	2.50	$[SiO_4]$:2.50
Ge^{4+}	0.50	4	2.00	$[GeO_4]$:2.00
Nb^{5+}	0.69	6	1.21	$[NbO_6]$:1.21

[a]Z denotes the valence number of cation.

in emission cross sections is dominantly caused by the difference in the Yb^{3+} site symmetries.

Clearly, if the difference of cationic field strengths among network formers in the systems with constant modifiers is high, the asymmetrical feature of the $[YbO_6]$ coordination sphere must be high. This in turn will be associated with an increase in the emission cross sections of Yb^{3+}. For example, since the difference in the cationic field strengths between the network formers as shown in Table III decrease in the order of B-Nb>P-Nb>Ge-B>Si-B, the values of emission cross sections for the Yb^{3+}-doped two-former systems with the nearly same ratios of former-1 to former-2 in the glasses increase in the order of Nb_2O_5-B_2O_3-RO>P_2O_5-Nb_2O_5-RO>GeO_2-B_2O_3-RO>SiO_2-B_2O_3-RO as shown in Table II.

It is well known that most of the f-f transitions of trivalent lanthanides have intensities which are little affected by the environment of the ion. A few, however, are very sensitive to the environment, especially of the symmetry of rare-earth ligand and are usually more intense when the ion is complexed than they are in the corresponding aquo ions. Such transitions have been called "hypersensitive transitions" by Jørgensen and Judd.[17] When a ion is at a center of symmetry, the intensity of its hypersensitive transition is zero, but small deviations from the ion site symmetry can cause the hypersensitivity to have quite large intensity while leaving the intensities of the other transitions virtually unaltered.[18] Based on these characteristics of the hypersensitive transition, the correlation of the Yb^{3+} site symmetry with glass composition may be understood from variation behavior of a known hypersensitive transition of a rare-earth ion, for example, the $^4I_{9/2}$-$^2G_{7/2}$ transition of Nd^{3+},[19] with the glass composition. Figure 4 shows the measured absorption spectra of Nd^{3+} in the P_2O_5-Nb_2O_5-RO system, in which the Nb_2O_5 concentration is varied from 0 to 20 mol %. Replacing the P_2O_5 by the Nb_2O_5, the intensity of the $^4I_{9/2}$-$^2G_{7/2}$ hypersensitivity strongly increases, but the intensities of the other transitions are practically unaltered. It proves that the addition of Nb_2O_5 for replacing P_2O_5 considerably enhances the asymmetry of rare-earth ligand. Comparing the absorption properties of Yb^{3+} and Nd^{3+} ions, the $^2F_{7/2}$-$^2F_{5/2}$ transition can be considered as an hypersensitive transition, since its oscillator strength strikingly increases as well as that of the $^4I_{9/2}$-$^2G_{7/2}$ transition with increasing the Nb_2O_5 concentration as shown in Fig. 5.

The potential performance of an Yb laser generally requires the emission cross section to be large at the laser

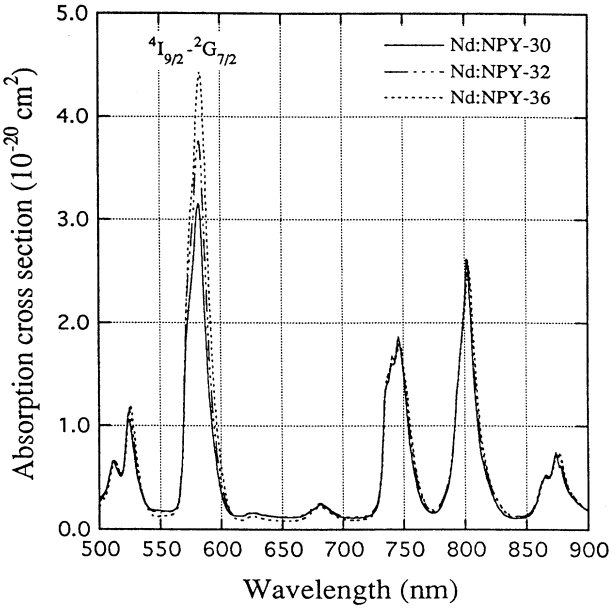

FIG. 4. Absorption spectra of Nd^{3+} in $(45-x)P_2O_5$-xNb_2O_5-24CaO-10SrO-20BaO (mol %) glasses doped with 1 mol %Nd_2O_3(x=0, 10, and 20).

wavelength for pulsed excitation, although the actual magnitude that is most useful may depend on the pulse length, pumping conditions, damage threshold, and other factors. A large cross section is also useful for cw operation, especially of the product of the emission cross section and the lifetime that plays key role. Here we suggest that the I_{min}, σ_{emi}, and $\sigma_{emi}\tau_f$ parameters together provide a good spectroscopic measure of the overall usefulness of the laser medium for the pulse or the cw operation. The I_{min}, σ_{emi}, and $\sigma_{emi}\tau_f$ values

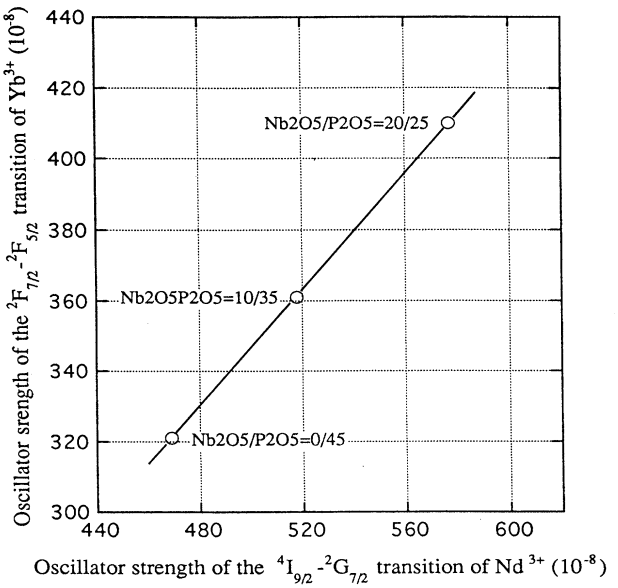

FIG. 5. Oscillator strengths of the $^4I_{9/2}-{}^2G_{7/2}$ transition of Nd^{3+} and the $^2F_{7/2}$-$^2F_{5/2}$ transition of Yb^{3+} in $(45-x)P_2O_5$-xNb_2O_5-24CaO-10SrO-20BaO (mol %) glasses (x=0, 10, and 20).

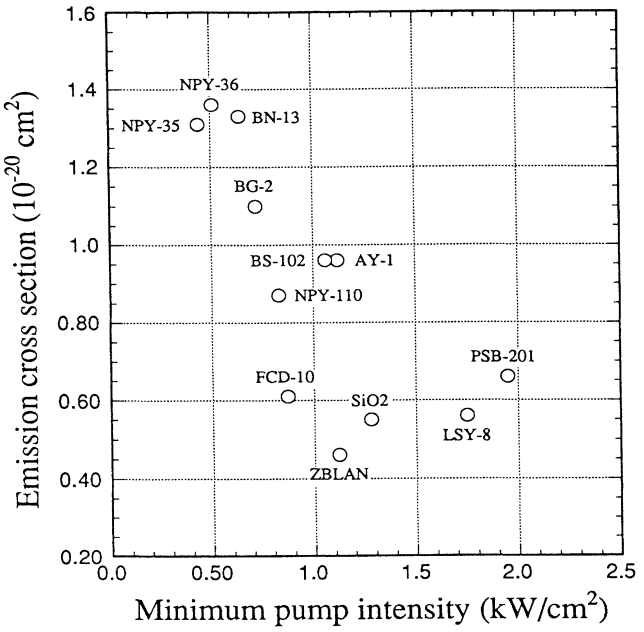

FIG. 6. A plot of emission cross section versus minimum pump intensity of Yb^{3+} for the selected glass hosts from the given systems.

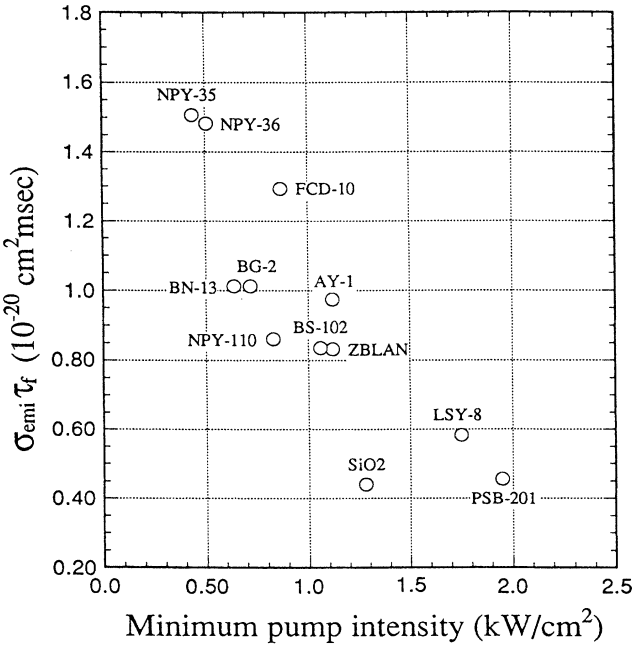

FIG. 7. A plot of the product of emission cross section, σ_{emi}, and emission lifetime, τ_f, versus minimum pump intensity of Yb^{3+} for the selected glass hosts from the given systems.

of the optimum glasses selected from the given systems are plotted in Figs. 6 and 7. It is generally desirable for σ_{emi} to be as large as possible to provide moderate gain, for τ_f to be long to minimize the pump losses incurred from normal emission, and for I_{min} to be small. This criterion serves to minimize the threshold for an Yb-laser material engaged in an oscillator-type configuration, and also to offer the best extraction efficiency at the laser wavelength, 1.02 μm. It is apparent from Figs. 6 and 7 that the Yb^{3+}-doped PNB-18 and PN-20 glasses are the most favorable materials when judged on this basis. It is interesting that Yb:PNB-18 and Yb:PN-20 appear to uniquely occupy a superior domain in the parameter space than do the other glasses involving Yb:SiO_2 and Yb:ZBLAN glasses. Both the glasses are desirable for the gain mediums to be compatible with AlGaAs or InGaAs diode pump sources and to have the higher laser efficiency.

V. CONCLUSION

The emission cross sections of Yb^{3+}-doped glasses are determined from the measured absorption spectra using both methods based on the principle of reciprocity and Fuchtbauer-Ladenburg formula. The absorption and emission properties of the $^2F_{7/2}$-$^2F_{5/2}$ transition are very sensitive to the Yb^{3+} site environments as well as an hypersensitive transition. Their magnitudes increase as the Yb^{3+} site asymmetry becomes higher. High asymmetry of the Yb^{3+} sites results not only from larger difference in the cationic field strengths among network formers surrounding [YbO_6] octahedrons, but also from difference in the coordination numbers of oxygens surrounding the network formers which are neighbored with the Yb^{3+} ions.

The spectral properties relevant to the predicted laser performance establish the ease of pumping the laser material and the I_{min}, σ_{emi}, and $\sigma_{emi}\tau_f$ parameters, taken together effectively, can describe the usefulness of the laser medium. Since it is desirable to have higher values of σ_{emi} and $\sigma_{emi}\tau_f$, and lower values of I_{min}, the Yb^{3+}-doped (15–25) P_2O_5-(10–20) Nb_2O_5-(0–15) B_2O_3-(48–55) RO (R=Mg, Ca,Sr, Ba, and Zn) (mol %) glasses are judged to be unique host materials for 1.02 μm Yb-fiber laser and Yb-high power laser.

[1] Y. Durteste, M. Monerie, J. Y. Allain, and H. Poignant, Electron. Lett. **27**, 626 (1991).

[2] S. F. Carter, D. Szebesta, S. T. Davey, R. Wyatt, M. C. Brierley, and P. W. France, Electron. Lett. **27**, 628 (1991).

[3] Y. Ohishi, T. Kanamori, T. Kitagawa, S. Takahashi, E. Snitzer, and G. H. Sigel, Opt. Lett. **27**, 1747 (1991).

[4] Y. Ohishi, T. Kanamori, M. Shimizu, M. Yamata, Y. Terunuma, J. Temmyo, M. Wata, and S. Sudo, IEICE Trans. Commun. **E77-B**, 421 (1994).

[5] Y. Ohishi, T. Kanamori, J. Temmyo, M. Yamata, M. Shimizu, K. Yoshino, H. Hanafusa, M. Horiguchi, and S. Takahashi, Electron. Lett. **27**, 1995 (1991).

[6] J. Y. Allain, M. Monerie, and H. Poignant, Electron. Lett. **27**, 1012 (1991).

[7] Y. Ohishi, T. Kanamori, T. Nishi, S. Takahashi, and E. Snitzer, IEEE Photon. Technol. Lett. **3**, 990 (1991).
[8] D. C. Hanna, R. M. Percival, I. R. Perry, R. G. Smart, P. J. Suni, J. E. Townsend, and A. C. Tropper, Electron. Lett. **24**, 1111 (1988).
[9] J. R. Armitage, R. Wyatt, B. J. Ainslie, and S. P. Craig-Ryan,Electron. Lett. **25**, 298 (1989).
[10] J. Y. Allain, M. Monerie, and H. Poignant, Electron. Lett. **28**, 988 (1992).
[11] J. Y. Allain, J. F. Bayon, M. Monerie, P. Bernage, and P. Niay, Electron. Lett. **29**, 309 (1993).
[12] D. E. McCumber, Phys. Rev. **136**, A954 (1964).
[13] A. Brenier, C. Pedrini, B. Moine, J. L. Adam, and C. Pledel, Phys. Rev. B **41**, 5364 (1990).
[14] S. A. Payne, L. L. Chase, L. K. Smith, W. L. Kway, and W. F. Krupke, IEEE J. Quantum Electron. **QE-28**, 2619 (1992).
[15] L. D. Deloach, S. A. Payne, L. K. Smith, W. L. Kway, and W. F. Krupke, J. Opt. Soc. Am. B **11**, 269 (1994).
[16] T. Kokubo, Y. Inaka, and S. Sakka, J. Non-Cryst. Solids **81**, 337 (1986).
[17] C. K. Jørgensen and B. R. Judd, Mol. Phys. **8**, 281 (1964).
[18] R. D. Peacock, in *Structure and Bonding*, edited by J. D. Dunitz *et al.* (Springer-Verlag, Berlin, 1975), Vol. 22, p. 83.
[19] A. F. Kirby and R. A. Palmer, Inorg. Chem. **20**, 1030 (1981).